药明康德
WuXi AppTec

WuXi Biology

CASE STUDY

CLINICAL RELEVANCE OF NASH ANIMAL MODELS

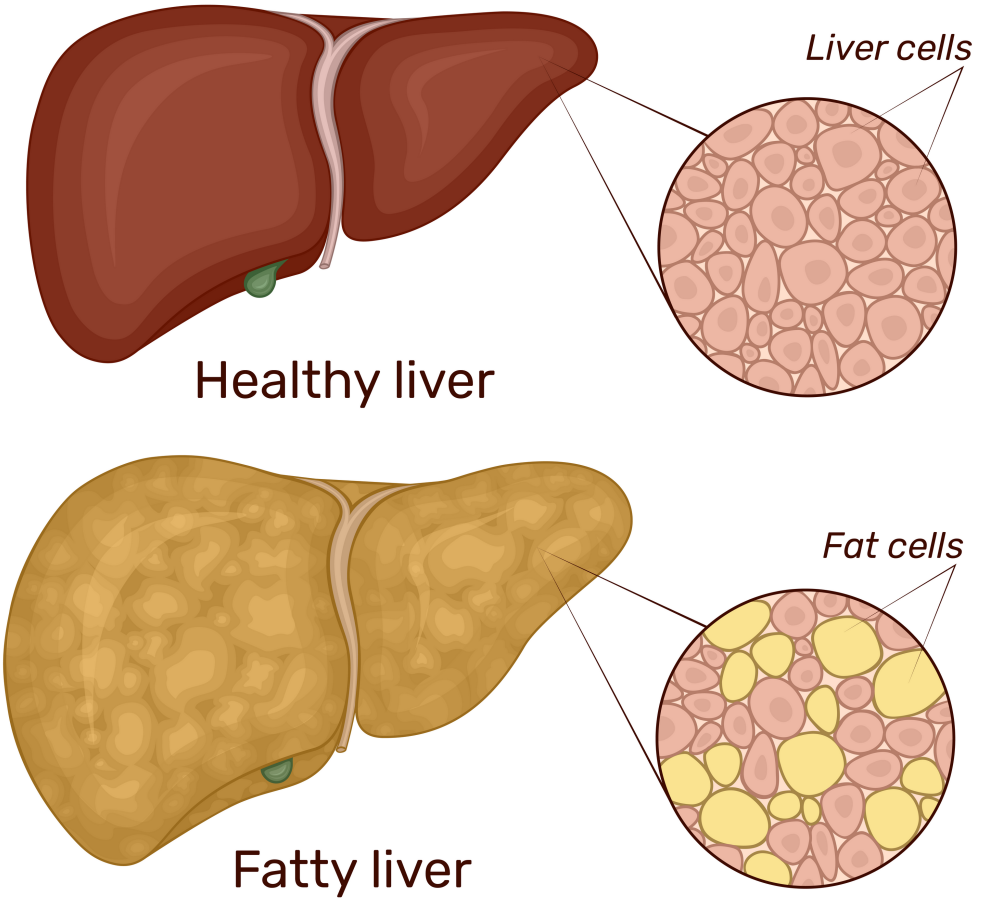

Clinical Relevance of NASH Animal Models:

An Animal Case for Resmetirom and Obeticholic Acid

Obeticholic acid (OCA) and resmetirom (RES) are the only compounds that completed phase 3 clinical trials and met their respective endpoints for treatment of non-alcoholic steatohepatitis (NASH). Given the low success rate of NASH compounds in clinical trials, the preclinical efficacies in animal models for NASH are a conundrum if not a confounding complication. Indeed, the conflicting in vivo efficacy results from animal models challenge the validity and the clinical relevance of any animal model claimed to be that of NASH.

A case in point, when OCA and selonsertib (SEL) were tested in the MCD (methionine and choline deficient diet) model in mice, OCA improved only steatosis, while the latter showed efficacy in improving all histopathological features related to NASH (Figure I-A). However, in the phase 3 clinical trial STELLAR-4, SEL did not meet the endpoints (Figure I-B).

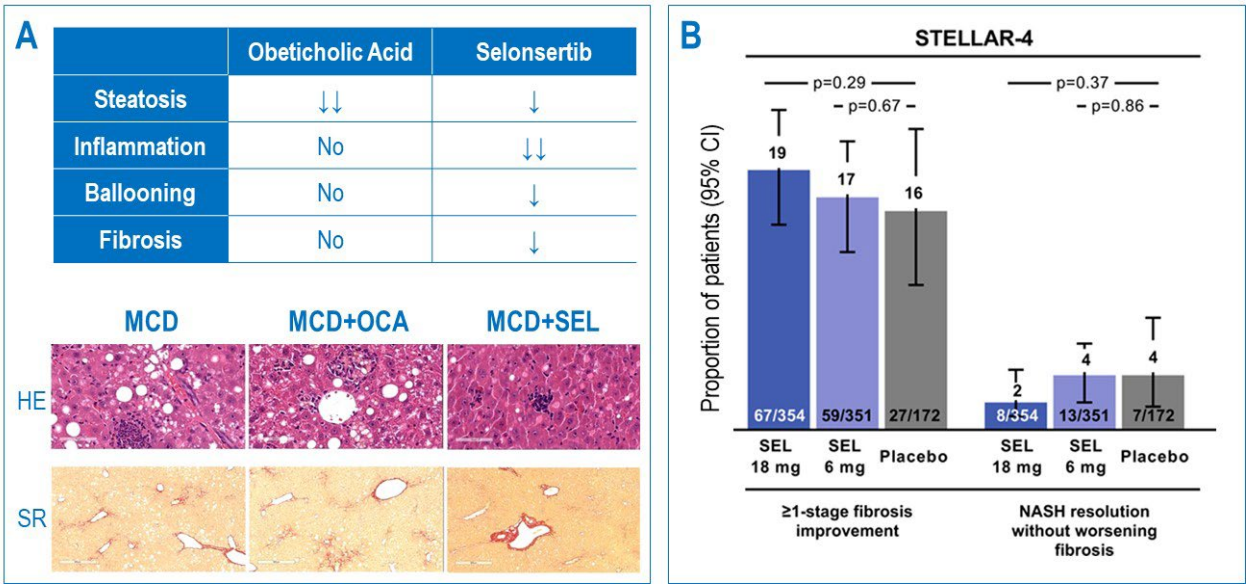

Figure I. **A. In vivo efficacy test of obeticholic acid and selonsertib in the MCD mouse model**. Top, summary of efficacies of OCA and SEL on 4 NASH-related histopathological features, ↓ indicating significant reduction. Bottom: liver slices of MCD animals treated with OCA and SEL stained with HE and Sirius red (SR) (Source, WuXi internal results). **B. Clinical outcome of SEL in STELLAR-4**. (Harrison et al. 2020. *J. Hepatol.* **73**:26).

On the other hand, in the AMLIN model, RES improved, on average, the NAS (NAFLD activity score, the sum of steatosis, inflammation and ballooning scores) by 1.6 out a total of 5.8), with no effects on fibrosis (Figure II, Kannt et al., 2021, *Br J Pharmacol*, **178**:2412). However, in the phase 3 trial MEASTRO-NASH, RES met the 2 primary endpoints, 1) NASH resolution with ≥2 point reduction in NAS and no worsening of fibrosis; and 2) ≥1 stage improvement in fibrosis with no worsening of NAS, and the key secondary endpoint of lowering blood LDL-C after 24 weeks of treatment (source: madrigalpharma.com).

These two confounding efficacy studies in two animal models (and other studies in other models) raise the question as to whether such an animal model exists of which the in vivo efficacy results are reflective of the clinical outcomes of any NASH compounds in question.

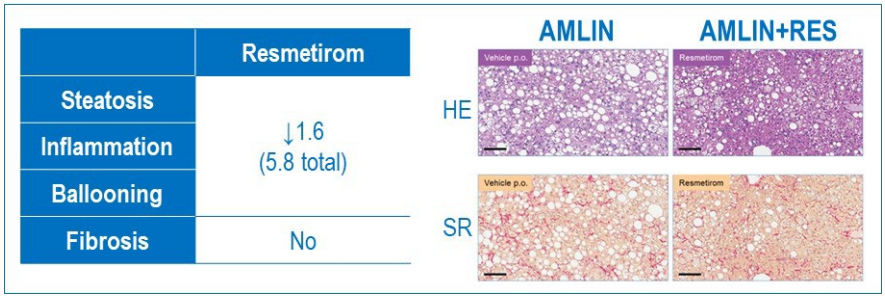

Figure II. **In vivo efficacy of resmetirom (RES) in the AMLIN model**. Left, summary of efficacy on NAS (sum of steatosis, inflammation and ballooning) and fibrosis. Right, HE and Sirius red staining of livers of the AMLIN animals treated with RES. (Adapted from Kannt et al., 2020).

The HFD+CCL4 (high-fat diet and carbon tetrachloride) model is a composite of HFD-induced steatosis followed by subsequent CCL4-induced fibrosis. In this model, we tested 5 NASH compounds that were in clinical trials with variable outcomes: obeticholic acid (OCA), resmetirom (RES), selonsertib (SEL), cenicriviroc (CVC) and elafibranor (ELA, Figure III).

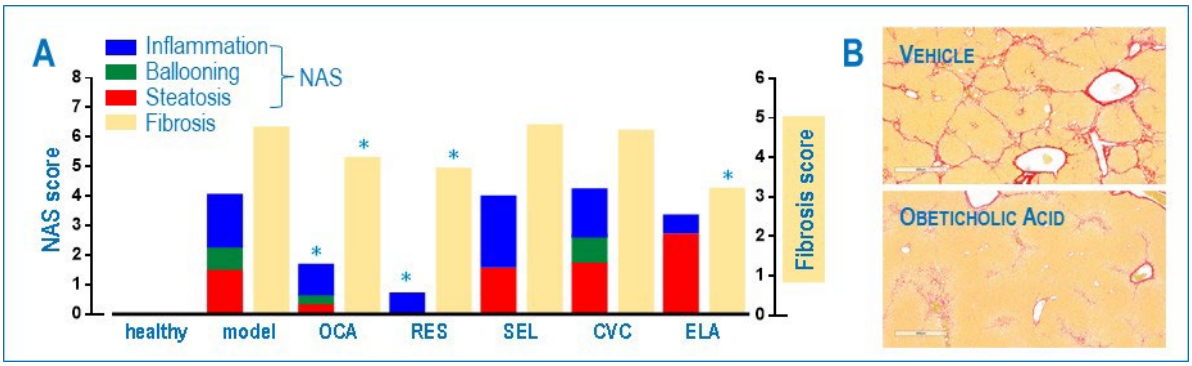

Figure III. **A. In vivo efficacies of 5 NASH compounds in the HFD+CCL4 model**. Asterisks indicate statistical significance vs. the model control. **B. Sirius red staining of liver slices from the model animals treated with vehicle (top) and obeticholic acid (bottom)**.

In this model, both OCA and RES displayed significant efficacy in improving NAS and fibrosis. In particular, steatosis was strongly suppressed by both compounds, while RES also reduced markedly hepatic inflammation and ballooning of hepatocytes. On the other hand, both compounds reduced fibrosis by a score ~1 (but consistently so) (Figure III-A). SEL improved ballooning with no effect on steatosis or fibrosis, but enhanced inflammation. CVC exerted no effect on any of histopathological features, whereas, ELA increased the level of steatosis while reducing inflammation, ballooning and fibrosis (Figure III-A).

In the same study, RES significantly reduced the blood levels of triglyceride (TG), total cholesterol (TC), LDL-cholesterol (LDL-C) and HDL-cholesterol (HDL-C) (Figure IV), consistent with clinical findings that this compound improved blood LDL-C in heathy and NASH individuals. OCA, however, improved only the blood level of LDL-C in this model. SEL and CVC had little or no

significant effect on the blood levels of these 4 biomarkers. ELA increased the blood levels of TC and LDL-C, consistent with the histopathological finding (Figure IV).

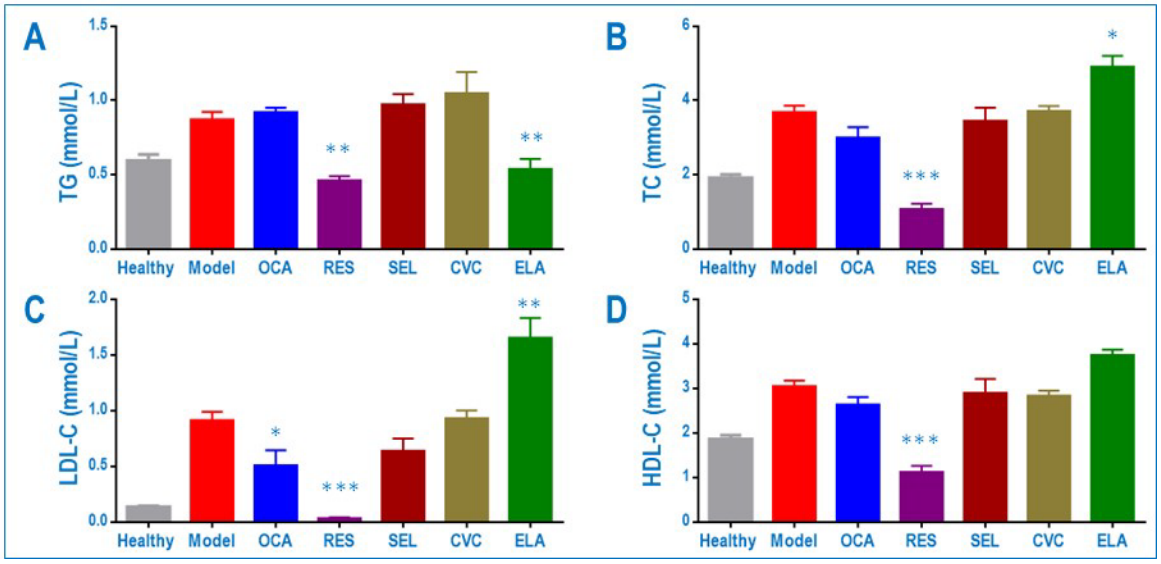

Figure IV. **Effect of 5 NASH compounds on the blood levels of TG, TC, LDL-C and HDL-C in the HFD+CCL4 model.**

Table I. Comparison of the clinical outcomes of 5 NASH compounds with their in vivo efficacy in the HFD+CCL4 model.

NASH Compound	Target	Phase III Trial Endpoint	Efficacy in HFD+CCL4 Model	
			Histopathology	Blood Biochemistry
Obeticholic acid OCA	FXR agonist	REGENERATE-ITT* | YES | 2018.10	✓	Partial
		REVERSE** | NO | 2022.10		
Resmetirom RES	THR-β agonist	MEASTRO | YES | 2022.12	✓	✓
Selonsertib SEL	ASK1 inhibitor	STELLAR-4 | NO | 2019.02	NO	NO
Cenicriviroc CVC	CCR2/CCR5 inhibitor	AURORA | NO | 2021.01***	NO	NO
Elafibranor ELA	PPARα/δ inhibitor	RESOLVE-IT | NO | 2022.08***	NO	✓

* ITT = intend-to-treat NASH; ** for treatment of advanced cirrhosis associated with NASH; *** terminated. (Source: clinicaltrials.gov)

The in vivo efficacy results, as determined by histopathological features (NAS and fibrosis) of these 5 NASH compounds in the HFD+CCL4 model are largely consistent with the respective outcomes in phase 3 clinical trials (Table I). In what follows, we describe how this animal model was characterized and how its clinical relevance was determined. In short, our results demonstrate that the in vivo efficacy observed in the HFD+CCL4 model is reflective of the clinical outcome.

The choice of NASH (nonalcoholic steatohepatitis) animal models has been a challenge for in vivo efficacy testing of compounds at various stages of development. We explored several rodent models, including high-fat diet + carbon tetrachloride (HFD+CCL4), methionine-choline deficient (MCD), choline-deficient high fact diet (CDHFD), choline deficient and defined amino acids (CDAA), high-fat diet with fructose and glucose (HFD+FRU/GLU), Amylin diet, and streptozotocin + high-fat diet (STZ+HFD). Here we selected two such models, HFD+CCL4 and MCD, for comparison to assess their performances in efficacy studies.

Both models are based on metabolic induction with different durations (Figure 1A). Whereas the HFD+CCL4 model is a sequential induction, high-fat diet followed by CCL4 induction, the second model is induced by the MCD diet. In the HFD+CCL4 model, test compounds are administered concomitantly with CCL4 induction. In the MCD model, test compounds are dosed in the second half of the 8-week induction period (Figure 1A).

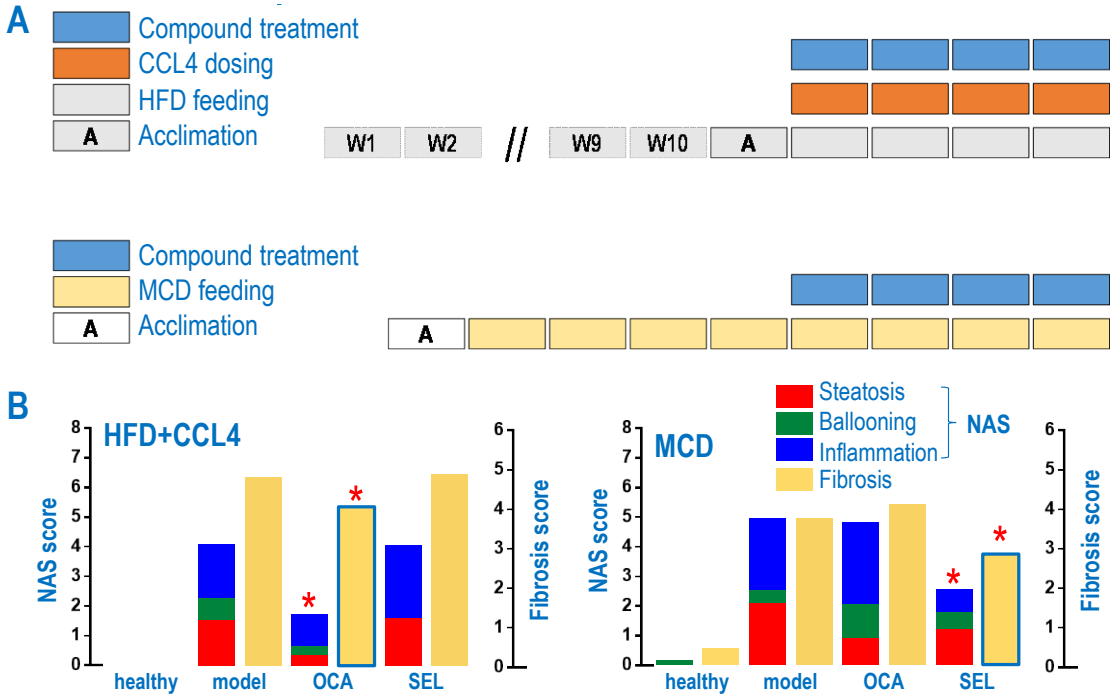

Figure 1. A. Schematic representation of HFD+CCL4 (top) and MCD (bottom) models, with compound treatment highlighted, and each box representing one week duration. B. Histopathological results of efficacy studies of obeticholic acid (OCA) and selonsertib (SEL) in HFD+CCL4 (*left*) and MCD (*right*) models. NAS (Non-Alcoholic Fatty Liver Disease Activity Score) is a composite of three histopathological findings found in the livers of the NASH patients, steatosis, ballooning and inflammation (scores of 3, 2 and 3, respectively). The clinical scoring of hepatic fibrosis is also adopted (total score of 5). Red asterisks indicate statistical significance compared with the model, and blue box outline indicates significant reduction in fibrosis.

Two compounds in NASH clinical trials (at the time the experiments were performed), obeticholic acid (OCA) and selonsertib (SEL), were tested in both models (Figure 1B). In the

HFD+CCL4 model, OCA reduced NAS by a margin of 3-4 score and fibrosis by score of 1, both of which are statistically significant. In particular, OCA reduced steatosis and inflammation significantly. However, SEL showed no improvement on NAS or fibrosis. On the contrary, the reverse was observed in the MCD model; i.e., only SEL reduced significantly NAS and fibrosis.

We used whole-liver RNA-seq to analyze the transcriptional responses in both models treated with OCA and SEL (Figure 2). When all the RNA transcripts were compared, the correlation between these two models was low, with an *r* value of 0.38. This correlation was further reduced when comparing transcripts involved in inflammation and lipid metabolism, with *r* values of 0.05 and 0.31, respectively, suggesting these two models are mechanistically different. This is particularly true for the hepatic inflammation components of both models.

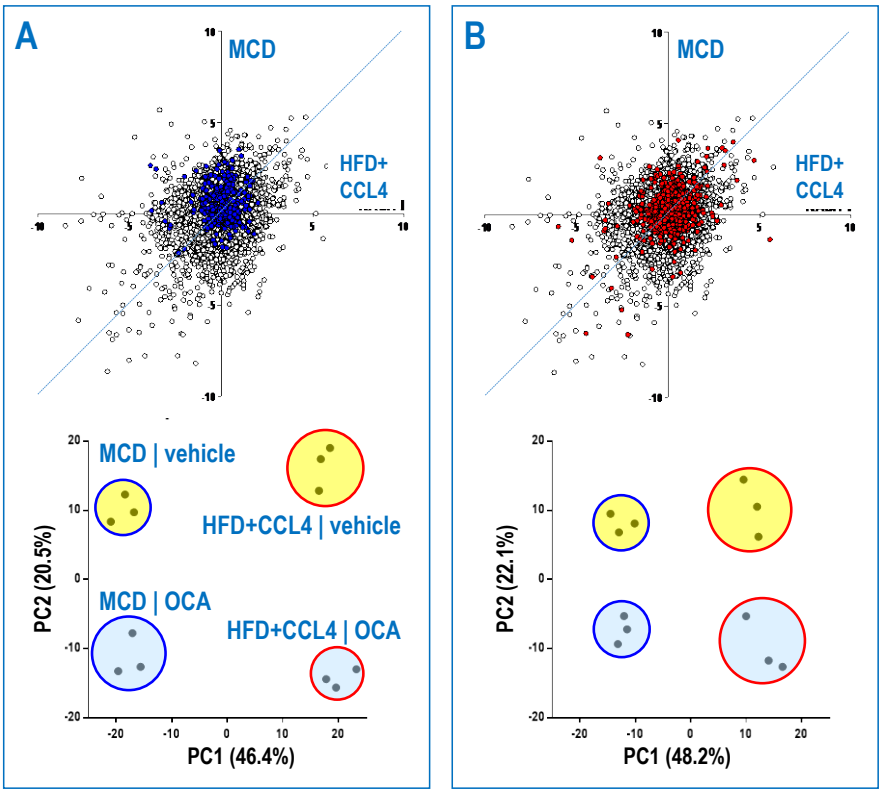

Figure 2. Comparison of the transcription profiles (by whole-liver RNA-seq) of HFD+CCL4 and MCD models. Shown on the top are the scatter plots of normalized z-scores (positive, up-regulated; negative down-regulated) of all transcripts (open circles), those involved in inflammation (blue dots, A) and lipid metabolism (red dots, B) in HFD+CCL4 (*x*-axis) and MCD (*y*-axis) models. The overall correlation coefficients (*r* values) are 0.38, 0.05 and 0.31 for all transcripts, those involved in inflammation, and those involved in lipid metabolism, respectively. Shown at the bottom are the principal component analysis plots of regulation of transcription of genes involved in inflammation (A) and lipid metabolism (B) in HFD+CCL4 (red circles) and MCD (blue circles) treated with vehicle (yellow filling) and OCA (light blue filling).

When principal component analysis (PCA) was used to compare transcriptional responses of genes involved in inflammation and lipid metabolism, it became evident that these two models are quite different in these two aspects, with no overlap. The treatment of OCA resulted in changes in gene expression based on the original animal model (Figure 2).

In the HFD+CCL4 model, steatosis is induced by high-fat diet (with significant increase in body weight, i.e., obesity), and subsequent fibrosis is induced by CCL4. The lack of choline in the MCD model impairs export of triglycerides from hepatocytes, resulting in steatosis (due to accumulation of intracellular triglycerides) but without obesity – to the contrary, the MCD animals lose body weight due to lack of the essential animal acid methionine. Methionine is an antioxidant shown to improve cellular oxidative balance and mediate oxidative stress. The lack of methionine contributes to inflammation and fibrosis in the MCD model, the former of which is different from that in the HFD+CCL4 model. The differences in induction mechanisms were clearly reflected in the histopathological findings of livers in both animal models (Figure 3).

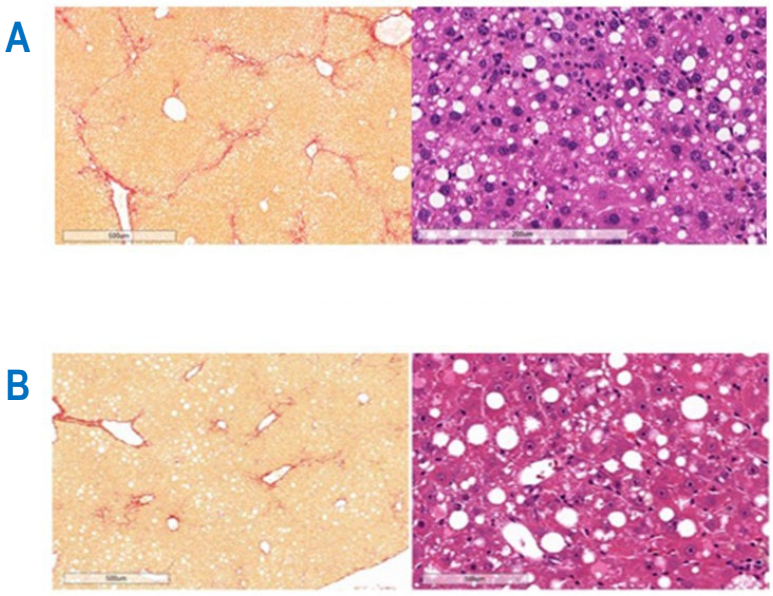

Figure 3. Histopathology of livers from the HFD+CCL4 (A) and MCD (B) models, stained with Sirius red (left) and HE (right). The selected fields are of the same scale.

The steatosis and fibrosis in these two models were morphologically different (Figure 3). Although the size of fat droplets varied in both models, the large droplets in the MCD model appeared considerably larger than those in the HFD+CCL4 model. Whereas fibrosis in the latter was more pronounced and structured as fibers, it was much less so in the MCD model (Figure 3).

To understand the fibrosis in the HFD+CCL4 model in relation to liver anatomic structure, we took advantage of a machine learning digital histopathology technology based on second harmonic generation/two photon excitation (SHG/TPE) microscopy (www.histoindex.com) to analyze and quantify the zonal distribution of hepatic fibrosis (Figure 4). In the analysis, the fibrosis in three hepatic zones, portal tract (zone 1), perisinusoidal space (zone 2) and central vein (zone 3), was positively recognized and quantified. Compared with the healthy control, the increase of fibrosis in zone 2 was greater than those in zones 1 and 3 in the model liver. After the treatment of OCA, the levels of fibrosis in zones 1 and 2 were significantly reduced, while the zone 3 fibrosis was largely unchanged. In contrast, SEL did not change the fibrosis in any of the three zones (Figure 4).

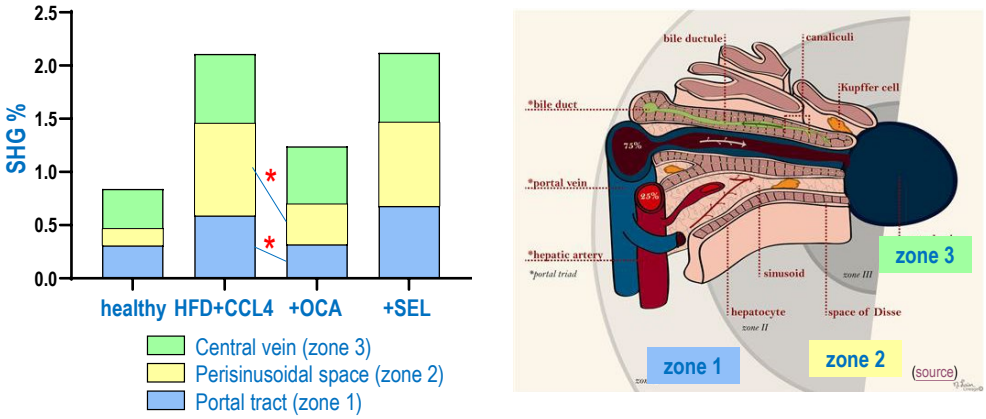

Figure 4. Quantitative histopathological analysis of hepatic fibrosis by second harmonic generation/two photon excitation (SHG/TPE) microscopy of unstained slices (in collaboration with HistoIndex). *Left*: quantification of fibrosis (SHG%) in three anatomic regions of liver from healthy animals, and the HFD+CCL4 animals with treatment of OCA and SEL. Red asterisks indicate statistical significance of reduction of fibrosis in perisinusoidal and portal track after OCA treatment. *Right*: Schematic illustration of liver zonal structure (diagram source: https://step1.medbullets.com/).

A more thorough comparison of the HFD+CCL4 and the MCD models reveals that the hepatic fibrosis in the former was structured as fiber strings in the portal tract and the perilobular regions. Bridging fibrosis was also evident in the HFD+CCL4 model. However, the fibrosis in the MCD model did not form recognizable fibers in these regions. Nor was bridging fibrosis found (Figure 5A). In fact, a comparison of various rodent models with hepatic fibrosis reveals that the mouse HFD+CCL4 and rat (and mouse) CDHFD (choline-deficient high-fat diet) models were the only ones with similar fibrosis (Figure 5B).

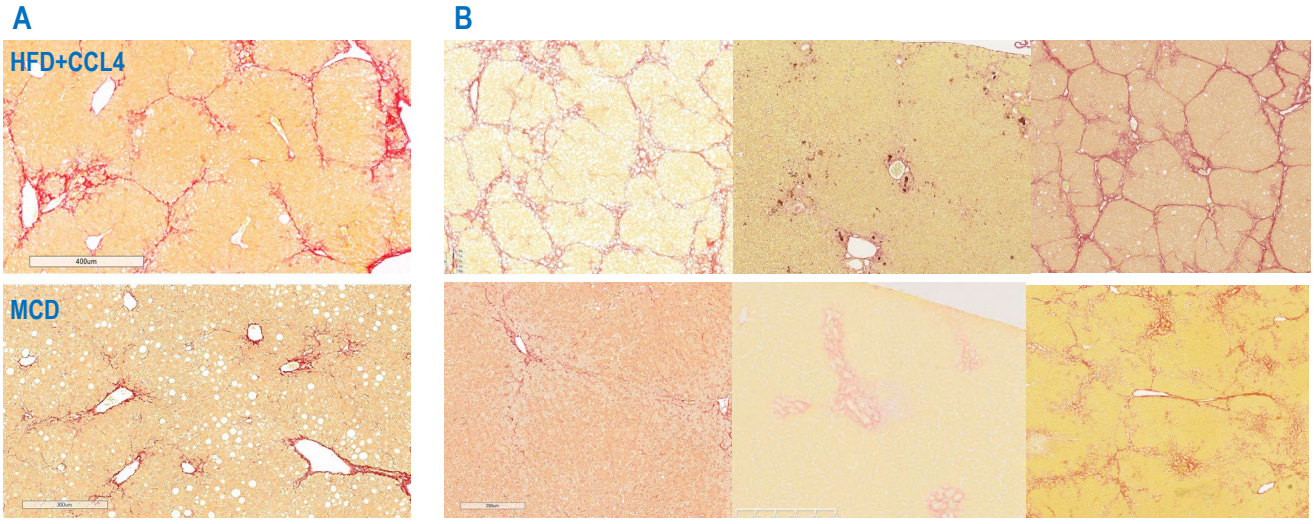

Figure 5. A compilation of hepatic fibrosis in rodent models. A. HFD+CCL4 and MCD models. B. Other rodent models with hepatic fibrosis, top left: CDHFD model.

Using the same digital histopathology method, the association of fibrosis with steatosis was analyzed in the HFD+CCL4 model treated with vehicle and OCA (Figure 6). As a control, the fibrosis induced by CCL4 alone was included in the analysis. Since CCL4 does not induce steatosis, only a

small fraction of the fibrosis was associated with the basal steatosis. However, in the HFD+CCL4 model, ~40% of the total fibrosis was found to be associated with steatosis. After OCA treatment, that portion of the fibrosis was reduced almost to basal level, while the rest of the fibrosis (steatosis-free) was slightly increased, by ~20% (Figure 6). These results suggest that the anti-fibrotic activity of OCA was exerted on fibrosis associated with steatosis. This was the first time such a mechanistic observation had been made in any animal models of NASH.

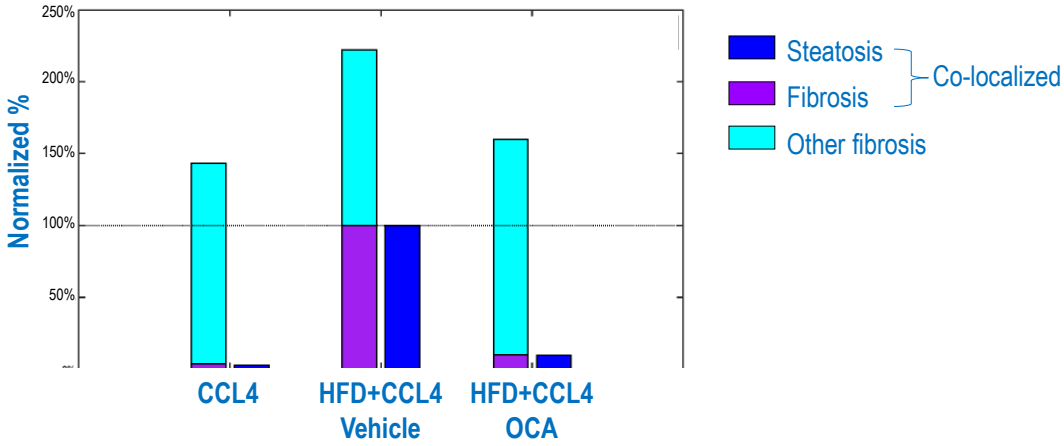

Figure 6. Quantitative histopathological analysis of fibrosis associated with steatosis in CCL4 induction (only fibrosis) and HFD+CCL4 model with vehicle and OCA treatment. In this analysis, the fibrosis associated with steatosis in the HFD+CCL4 model was normalized as 100%. Only steatosis associated with fibrosis (normalized as 100%) was analyzed.

We then tested additional NASH compounds in clinical trials in the HFD+CCL4 model (Figure 7 and Table 1). In one study, five compounds were tested, including OCA, SEL, cenicriviroc (CVC), elafibranor (ELA), and resmetirom (RES). Their molecular targets range from FXR, ASK1, CCR2/CCR5, PPAR-α/δ to THR-β. The results of OCA and SEL are described above. CVC displayed no activities against NAS or fibrosis, whereas RES ablated steatosis and ballooning, and reduced inflammation and fibrosis with statistical significance. On the other hand, elafibranor was active only against fibrosis and inflammation, but the steatosis was increased after the treatment (Figure 7). Of these five compounds, OCA and RES displayed significant therapeutic efficacy against both NAS and fibrosis.

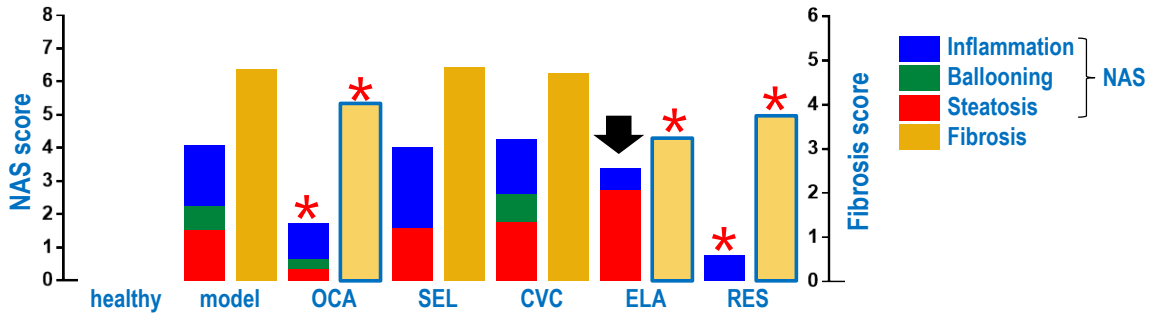

Figure 7. Efficacy tests of NASH compounds in clinical trials, obeticholic acid (OCA), selonsertib (SEL), cenicriviroc (CVC), elafibranor (ELA) and resmetirom (RES). Red asterisks indicate statistical significance; black arrow shows increase in steatosis.

Table 1. Summary of efficacy tests of NASH compounds in the HFD+CCL4 model

Compounds	Target	Efficacy Test Results [1]		Clinical Trial Status
		NAS	Fibrosis	
Obeticholic acid (INT-747)	FXR	Yes	Yes	P3, Completed [2]
Tropifexor (LJN452)	FXR	Yes	Yes	P2, Ongoing
Selonsertib (GS4997)	ASK1	No	No	P3, Failed
Elafibranor (GFT-505)	PPAR-α/δ	No	Yes	P3, Terminated
Lanifibranor (IVA337)	PPAR-α/δ/γ	Yes	Yes	P3, Ongoing
Cenicriviroc (TAK-652)	CCR2/CCR5	No	No	P3, Terminated
Resmetirom (MGL-3196)	THR-β	Yes	Yes	P3, Completed
VK2809	THR-β	Yes	Yes	P2b, Ongoing
Firsocostat (ND630)	ACC1/2	Yes	Yes	P2, Discontinued [3]
Liraglutide	GLP1	Yes	No	P2, Completed
Semaglutide	GLP1	Yes	No	P3, Ongoing
PXS 4728A	SSAO/VAP-1	No	No	P2, Discontinued
Aramchol	SCD-1	No	No	P3, Discontinued

Notes: **1**. Yes = improvement of NAS or fibrosis; **2**. In a previous trial, REGENERATE-ITT, OCA completed P3 trial with positive results. However, in a more recent trial, REVERSE, OCA failed to improve advanced fibrosis; **3**. Due to increase in blood triglycerides. The same observation was made in the HFD+CCL4 model.

Table 1 summarizes the results of efficacy tests of all the clinical NASH compounds in the HFD+CCL4 model. Compounds targeting THR-β (resmetirom and VK2809) and PPAR-α/δ/γ (lanifibranor) displayed therapeutic activities against both NAS and fibrosis in this model. These compounds have yielded positive results in the clinical trial so far. Likewise, both obeticholic acid and tropifexor displayed similar activities in this model. However, obeticholic acid completed an early trial (REGENERATE), but failed in a recent trial (REVERSE) due to lack of efficacy against advanced fibrosis. Compounds that failed or were discontinued in clinical trials (selonsertib, elafibranor, cenicriviroc, PXS4728A and aramchol) failed to improve NAS and/or fibrosis. With few exceptions, the efficacy results in the HFD+CCL4 model are largely consistent with the clinical outcomes of NASH compounds.

Firsocostat was efficacious in improving both NAS and fibrosis but caused an increase in blood triglycerides. A similar observation was made in the clinical trial, which was discontinued due to this reason. Liraglutide and semaglutide dramatically improved steatosis in this model but displayed no anti-fibrotic activity. Their clinical trials are still open.

Based on these results, we concluded that fibrosis in the HFD+CCL4 model bears certain relevance to that observed in NASH patients. However, the fibrosis induced by CCL4 alone was not the target of OCA (data not shown). Since the HFD+CCL4 model is a composite of HFD and CCL4 induction, we compared the histopathological findings of these three models (Figure 8).

HFD alone induced steatosis and inflammation, but no fibrosis. CCL4 induced inflammation, ballooning (among other hepatic damages) and fibrosis, but no steatosis. When the two were combined, all these histopathological findings were present in the model, and the level of fibrosis was further increased. After treatment of OCA, fibrosis was reduced to the level induced by CCL4 with statistical significance. It seems that the extra level of fibrosis (ΔF), induced when HFD and CCL4

were combined ($F_{[HFD+CCL4]} - F_{[CCL4]}$), was (quantitatively) the target of the anti-fibrotic activity of OCA ($F_{[HFD+CCL4 \mid OCA]} - F_{[HFD+CCL4]}$) (Figure 8). The latter ΔF has been consistently observed to be associated with the anti-fibrotic efficacy of OCA in ~100 studies with the HFD+CCL4 model in which the compound was used as a reference or quality control. These results suggest that ΔF induced in the HFD+CCL4 model is likely related to the fibrosis observed in NASH patients, i.e., this is likely a relevant NASH model. In addition to its anti-fibrotic efficacy, OCA was efficacious in improving the steatosis and the hepatic inflammation in this model. However, the compound did not show consistent efficacy against the ballooning (Figure 8), due likely to relatively large heterogeneity between individual animals (data not shown).

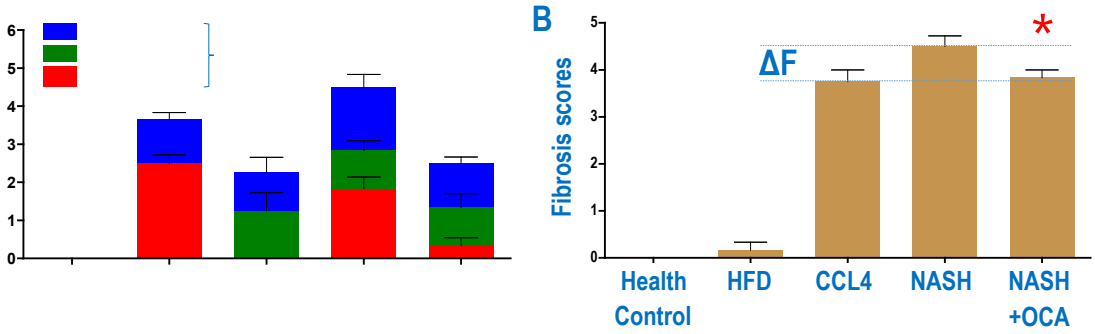

Figure 8. Deconstruction of HFD+CCL4 (NASH) model. The two components of the HFD+CCL4 model were tested along with OCA treatment in the same study. The NAS results are shown in A, and fibrosis in B. ΔF is the difference of fibrosis between HFD+CCL4 and CCL4 inductions, which has been shown to be approximately, but consistently, the difference between the model and treatment of OCA. Red asterisks indicate statistical significance between the model and the treatment.

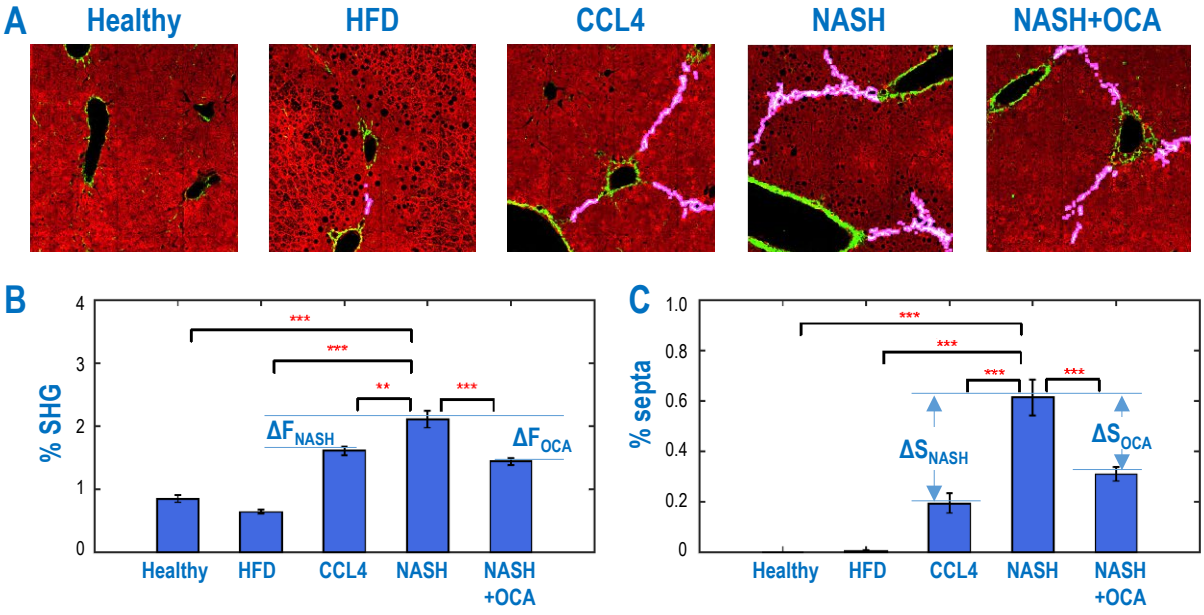

Figure 9. SHG/TPE digital histopathology and quantification of fibrotic septa in healthy control, HFD and CCL4 induction, and NASH (HFD+CCL4) model with and without OCA treatment. A. Representative fields of SHG/TPE microscopies, with fibrotic septa labeled in pink. B. Total fibrosis. C. Fibrotic septa. **, $p < 0.01$; ***, $p < 0.005$. For ΔF and ΔS, see text for full description.

Since bridging fibrosis, in the form of fibrotic septa, is a common histopathological finding associated with NASH patients and a feature that is recognized by the SHG/TPE digital histopathology (Figure 9A), we quantified the total fibrosis and the fibrotic septa in the HFD+CCL4 model and its constituent models (Figures 9B and 9C, Table 2). Consistent with the fibrosis score results, HFD+CCL4 significantly induced an extra level of total fibrosis (by ~55%) compared with CCL4 induction alone ($F_{[HFD+CCL4]} - F_{[CCL4]} = 0.5\%$, cf. $F_{[CCL4]} = 0.9\%$, with basal fibrosis subtracted). After OCA treatment, fibrosis was reduced to a similar level as in the CCL4 induction; i.e., $F_{[HFD+CCL4 \mid OCA]} - F_{[HFD+CCL4]} = 0.6\%$ cf. $F_{[HFD+CCL4]} - F_{[CCL4]} = 0.5\%$ (Figure 9B, Table 2). The anti-fibrotic efficacy of OCA ($\Delta F_{OCA} = F_{[HFD+CCL4 \mid OCA]} - F_{[HFD+CCL4]}$, quantified by SHG/TPE digital histopathology, was largely consistent with what was observed in a separate study shown in Figure 4.

Table 2. Quantification of total fibrosis (F, as determined by % SHG in Figure 9) and fibrotic septa (S, % septa) in CCL4 induction, HFD+CCL4 model, and HFD+CCL4 model with OCA treatment.

	CCL4	HFD+CCL4	HFD+CCL4 | OCA	ΔNASH [1]	ΔOCA [2]
F (total fibrosis % SHG)	0.9%	1.4%	0.8%	0.5%	0.6% (120%) [3]
S (fibrotic septa % septa)	0.2%	0.6%	0.3%	0.4%	0.3% (75%) [3]
Septa/Total	22%	43%	38%	80%	50%

Note: **1**. ΔNASH = [HFD+CCL4] – [CCL4]; **2**. ΔOCA = [HFD+CCL4 | OCA] – [HFD+CCL4]; **3**. ΔOCA/ΔNASH

Quantified by SHG%, basal levels of fibrosis were observed in the healthy control and HFD induction group (Figure 9B). In contrast, no significant fibrotic septa were seen in these two groups of animals (Figure 9C). While CCL4 induced the septa ($S_{[CCL4]} = 0.2\%$), the combination of HFD and CCL4 (NASH) significantly increased the induction of the fibrotic septa ($S_{[HFD+CCL4]} = 0.6\%$) (Figure 9C, Table 2). It was estimated that 80% of the ΔF seen in the HFD+CCL4 model ($\Delta F_{NASH} = F_{[HFD+CCL4]} - F_{[CCL4]} = 0.5\%$) was the fibrotic septa ($\Delta S_{NASH} = S_{[HFD+CCL4]} - S_{[CCL4]} = 0.4\%$); i.e., the combination of HFD and CCL4 induced largely the NASH-like fibrotic septa. In contrast, fibrotic septa constituted ~20% of the total fibrosis induced by CCL4, and ~40% in HFD+CCL4 model with and without OCA treatment (Table 2).

Of the extra 0.4% fibrotic septa induced by the combination of HFD+CCL4 (i.e., ΔS_{NASH}), OCA treatment reduced it to 0.3% (i.e., ΔS_{OCA}). On the other hand, while the combination of HFD and CCL4 induced 0.5% extra total fibrosis, OCA treatment resulted in 0.6% reduction in total fibrosis (Table 2).

In summary, our analyses demonstrated that the combination of HFD and CCL4 in the NASH model induced extra level of total fibrosis, of which 80% was fibrotic septa. OCA exerted its anti-fibrotic activities almost equally on both fibrotic septa and non-septum fibrosis in this model.

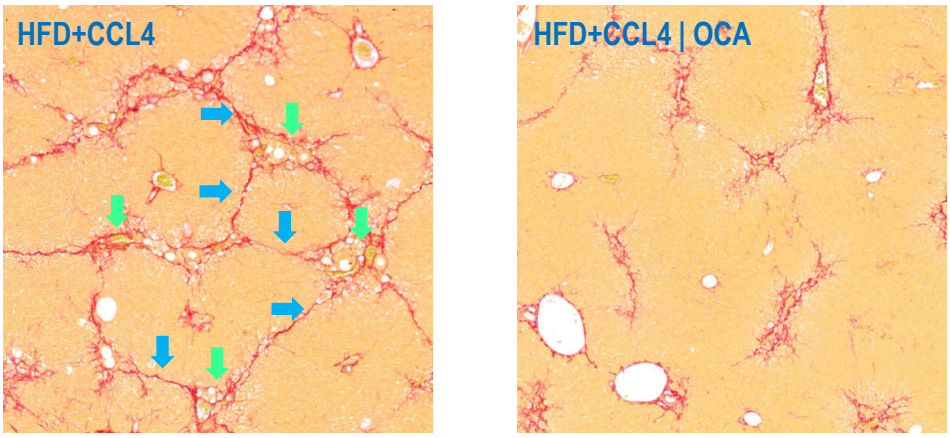

Figure 10. The anti-fibrotic activities of OCA in HFD+CCL4 model. The fibrosis in portal tract and perilobular regions are *highlighted* by green and blue arrows, respectively, in the NASH model *(left)*. The OCA treatment improves the fibrosis in these two regions *(right)*.

Improvement of hepatic fibrosis has been a challenging endpoint in NASH clinical trials. Selecting animal models to demonstrate anti-fibrotic efficacy has been equally challenging for the development and preclinical pharmacological research of NASH drugs. Our results demonstrate that not all hepatic fibrosis models are the same. In the case of HFD+CCL4 and MCD models, the histopathological findings in the former are more consistent with clinical observations. We arrive at this conclusion based on the results of efficacy studies of NASH compounds in clinical trials, which are largely consistent with their clinical outcomes (Table 1). The results shown in Figure 9 indicate strongly that the extra fibrosis induced in the HFD +CCL4 model is related to NASH clinical observations. Our analyses (Figures 4 and 9) further delineate the targets of the anti-fibrotic activities of OCA in the HFD+CCL4 model. As shown in Figure 10, the fibroid structures in two liver regions, the portal tract and perilobular septa, are likely the main targets of OCA. Combined with the results shown in Figure 6, we conclude that septum fibrosis associated with steatosis in the portal tract and perilobular regions are the main histopathological targets of OCA.

药明康德
WuXi AppTec

CONTACT US

WuXi AppTec Pharmacology Models for Liver Diseases

Acute liver injury models
- Alcohol induced acute liver injury models
- CCl4 induced acute liver injury models

Non Alcoholic steatohepatitis (NASH) / HCC models
- Fatty liver with NASH models in small and large animals (DIO + CCl4 / STZ + HFD)

Complicated factor induced chronic liver injury model
- High fat diet+alcohol+CCl4 induced liver fibrosis models in small and large animals

Chronic fatty liver models
- Obesity in liver damage models in small and large animals

Chronic liver injury models
- Multiple liver fibrosis/cirrhosis models in small and large animals

Endpoint Measurements
- Clinical observation and physical examination
- Biomarker analysis
- Histology analysis

LEARN MORE